International Journal on Recent and Innovation Trends in Computing and Communication
ISSN: 2321-8169 Volume: 11 Issue: 10
Article Received: *16 August 2023* ***Revised:*** *18 September 2023* ***Accepted:*** *20 October 2023*

Design An Intelligent System to Support Dental Cyst Detection Using Two Convolutional Neural Networks

Jinu Thomas[1], Dr. V. Ulagamuthalvi[2]
[1]Research Scholar, Department of CSE, Sathyabama Institute of Science and Technology, Chennai.
jinuullas2018@gmail.com
[2]Associate Professor Department of CSE, Sathyabama Institute of Science and Technology, Chennai,
ulagamv@gmail.com

Abstract— The aim of this paper is to develop a methodology, through studies on Computer Vision techniques, for the automatic identification of dental cysts in panoramic radiography images, providing Dental professionals with an alternative aid in the interpretation of these images. In addition segmentation techniques are applied in the inner region of the jaws, seeking to separate the regions with a greater possibility of cyst. The objective of this work is to design an intelligent system that supports the diagnosis of Dental Cyst using convolutional neural networks in order to help detect Dental Cyst at an early stage. The research method applied in this study consists of model design, where built and trained two convolutional neural network architectures, supporting 80% of the dataset with a total of 775 images with four image categories, and proposal validation, where we work with the remaining 20% of the dataset. Our results show that the ResNet50 architecture achieved the best classification with an accuracy of 98%.

Keywords-*Dental Cyst,Diagnosis,Classification,ConvolutionalNeuralNetworks.*

1.INTRODUCTION

The mouth is an important organ for the maintenance of life, functioning from a simple entrance of food for primitive beings to an organ of robust structure in more evolved organisms. In the latter group, it consists of a complex set of muscles, bones and nerves. For man, it offers several social and biological functions, acting in the body as an entrance to the digestive system in addition to assisting in breathing [1-2]. In the application of its biological function, caused by the entry of food, the oral cavity is also used as an entry and dwelling environment for viruses and bacteria, being one of the most populated habitats in the human body with about 6 million bacteria [3]. The presence of food remains and the characteristic of humidity makes this organ an ideal environment for the proliferation of these microorganisms that can cause different types of oral diseases. Mouth-related pathologies are present in a large part of the world's population and represent an important challenge for public authorities. According to the Global Burden of Disease 2017 study, carried out by the Institute for Health Metrics and Evaluation (IHME), the estimate of people with an incidence of oral diseases was 3.59 billion in 2017 [4-5], representing high growth compared to 2015 with 3.5 billion cases [6]. These data are obtained in 195 countries since 1990 and serve as a reference for the World Health Organization (WHO). Despite encouraging results, such as the reduction of cavities for some age groups, the research also showed that regional aspects impact these conditions [7]. Another condition presented by her is that there was a high incidence rate of other oral problems, demonstrating that these are still very present in the Brazilian population. Oral diseases also significantly impact the economy, whether with direct treatment costs or indirect ones, such as lost productivity at work. According to [8], the WHO estimates that the total economic impact of dental diseases in the world was U$ 442 billion in 2010. In the treatment of these diseases, the estimated world expenses are U$ 298 billion annually, representing an average of 4.6% of global health spending. Despite all investments in the treatment of oral diseases, the incidence remains high, with dental caries having the highest number of cases [9]. Another type of pathology that stands out is maxillary lesions, as they can present degenerative and proliferative characteristics with the potential to endanger the patient's life [10-11]. These lesions, which have specific clinical and radiographic characteristics, are relevant occurrences in oral and maxillofacial pathology [12]. Its incidences cause alterations in X-ray examinations, being divided into: odontogenic tumors, jaw cysts, pseudocysts, bone pathology and malignant neoplasms, the most frequent being tumors and cysts. The latter are more common in the dental clinic, while tumors are less frequent [13]. In clinical practice, odontogenic cysts are pathologies commonly encountered by radiologists. These can be detected by searching in places that show symptoms

indicated by patients or in some exam incidentally, which may represent a challenge to the diagnosis [14]. A recent study by [15], with data from 2006 to 2017 from the state of Bahia, shows that most intraosseous oral lesions are cystic, with a 47.5% incidence. Another survey by [16], in Rio Grande do Norte, found that the incident rate of odontogenic cysts was 11%, for exams collected over 38 years. These data show that odontogenic cysts have a considerable incidence in maxillary lesions, being the most frequent among intraosseous lesions.

2. RELATED WORK

Bearing in mind the need for early detection of cysts and the challenges offered by dental images, several VC studies have been developed in the search for algorithms that detect, segment and classify these pathologies [17-18]. These researches seek techniques and methodologies that obtain better results in aiding the diagnosis, either for a step of the CAD system or the complete process.

Literature [19] proposed a semi-automatic method to detect lesions in periapical X-ray images. The images are segmented into three regions, through two competitive level set functions. The input of these is an initial contour provided by the Support Vector Machine (SVM) classifier. With the segmented regions, an uncertainty map is created along with the average technique to select the most radiolucent areas, isolating the teeth and locating the lesions. The method was tested on 60 images and showed 9 False Positives (FPs) and 181 detected lesions.

Literature [20] proposed the use of Snakes for semi-automatic detection of dental lesions caused by cysts and tumors in panoramic radiographs. In the pre-processing, the Gaussian filter is used, in the segmentation step, a method based on the snake strain model is used, through modifications in the parameters related to energy weights and objective function. The method was applied to 24 images using initial positions provided by specialists and obtained an average accuracy of 99.67%.

Literature [21] performed a study on the analysis of cysts using texture information. Its methodology investigates pre-processing techniques and texture patterns for different types of cysts. In the first stage, block analysis, contrast extension and opening by reconstruction were tested. The texture used was obtained by GLCM statistics and parameters of contrast, correlation, energy, homogeneity and mean were evaluated. Tests were performed on 3 images, each with a different type of radiograph. The best pre-processing found was the contrastextension and the parameter that presents the greatest description among the types of cysts is energy.

Literature [22] developed a classification system for dental cysts in panoramic radiographic images. Its methodology consists of using a Gaussian filter to remove noise and perform the extraction of characteristics of the cysts through markings made by specialists. Extracted textures are based on First Order Statistics (FO), Gray Level Co-occurrence Matrix (GLCM), and Gray-Level Co-occurrence Matrix (GLRLM, from English Gray-Level Run Length Matrix). These were classified in an SVM and obtained better results for the combination of FO and GLRLM with an accuracy of 87.18% and an area under the Receiver Operating Characteristic (ROC) curve of 0.9444.

Literature [23] developed an automatic method for segmenting lesions in panoramic radiography images. An averaging filter is applied to the input image to attenuate noise. After that, the Fuzzy C-Mean with Neutrosophy is used to group it and obtain the degrees of association between the pixels. Integration with the logic of neutrosophy aims to reduce noise without blurring at the edges of images. Validation was tested on 95 images and the results obtained were 94.71% similarity, 95.92% sensitivity and 94.12% specificity, with a FPs ratio of 6.1%.

Literature [24] proposed an automated methodology for detecting periapical lesions caused by cysts or other factors, using panoramic radiography images. In this proposal, the mandibles are separated using the discrete wavelet transform with polynomial regression. After that, an angular radial sweep is performed to segment the teeth and locate the apex of the roots where the region growth will be applied. The method was tested on 9 images and obtained a sensitivity of 70% and a specificity of 89%.

Literature [25] proposed a hybrid automatic technique to detect and extract cystic regions using CNN. The proposed architecture results, with an accuracy of 0.9076, kappa of 0.7773, sensitivity of 0.8483, and specificity of 0.9321 and AUC of 0.8903, in the classification of pulmonary nodules.

Literature [26] developed a Convolutional Neural Network (CNN) for automatic detection of ameloblastomas and keratocysticodontogenic tumors. The database has 500 panoramic radiograph images. Images are pre-processed with inverse logarithm and histogram equalization. The architecture used is VGG-16 [27], which consists of 16 layers. This network was pre-trained with the ImageNet bank [28] and refined by training with the set of 400 exams. CNN was applied to 100 images and obtained an accuracy of 83%, specificity of 83.3% and sensitivity of 81.8%.

Literature [29] propose to evaluate the performance of lesion detection with deep learning in panoramic radiography images. The model was created using NVIDIA's DetectNet deep neural network with adaptive moment estimation (Adam)

International Journal on Recent and Innovation Trends in Computing and Communication
ISSN: 2321-8169 Volume: 11 Issue: 10
Article Received: *16 August 2023* ***Revised:*** *18 September 2023* ***Accepted:*** *20 October 2023*

and training with 500 epochs. 210 images are used in the training and the tests were performed with two groups, the first with 50 images from the training set and the second with 25 images not seen by the network. The results showed a sensitivity of 88% for both sets, with no FP in the first group and 0.04 FP/image in the second group.

Literature [30] proposed an automatic method to detect five types of cysts in panoramic radiography images. This uses a Deep Convolutional Neural Network (DCNN) obtained through modification of YOLO-v3 (REDMON; FARHADI, 2018) to detect odontogenic cysts. The latter presents pre-training done using the convolutional weights of the daknet53 model. The bank used consists of 1182 exams and from these, rotation, horizontal flip and gamma correction transformations were performed, increasing the number of images. The results showed a mean accuracy of detection (mAP) of 94.14%, precision of 0.99 and recall of 0.93.

Mentioned all of the above, in this work we propose to perform the segmentation of the images and then perform the diagnosis by applying convolutional neural networks

3. Dental Cyst Diagnostic System

In this section, the description of the contribution is made, which consists of developing a tool for the Diagnosis of Dental Cyst using Convolutional Neural Networks; the justification for the use of Convolutional Neural Networks, the map of the proposed model, as well as the general description and specification of each of its components are also part of this section.

3.1. Model

This section corresponds to the Model Phase of the research methodology mentioned in the previous section. This phase includes the dataset points, image preprocessing, and model training.

3.1.1. Data Set

The data set used for training the images from a study conducted in 460 patients. This dataset has 775 images divided into 2 types of cyst that are detailed in Table 1. In addition, Figure 1 shows the 2 types: Normal (Fig. 1(a)), Cyst (Fig. (1b)).

Table 1. Number of images

Image Type	Total
Normal	610
Cyst	160
Total	770

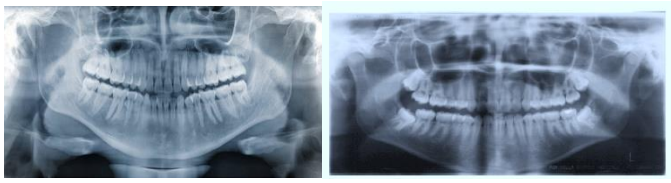

(a) Normal (b) Cyst

Figure 1 Example of images by type

To divide the set of images that will be used in the training and later in the validation, the Pareto Principle was used, 80% of the images will be used for training and the remaining 20% of the images will be used for validation, as shown in Table 2.

Additionally, from the number of training images, the Pareto principle was used again: 80% of the images will be used for training; and the remaining 20%, for the test.

Table 2 Division of images for training and validation

Image type	Training	Test	Validation	Total
Normal	390	100	120	610
Cyst	105	25	30	160
Total	495	125	150	770

3.1.2. Image preprocessing

For the preprocessing of the images, the k-means algorithm was used, which is an unsupervised algorithm, which is used for image segmentation based on centroids, this algorithm is provided by the Sklearn library, which is a library machine learning for the Python programming language.

In Figure 2, you can see the Original image (Fig. 2a) and the Segmented image (Fig. 2b) by the algorithm on the right. For this case study, the K-means algorithm was used with the value of 3.

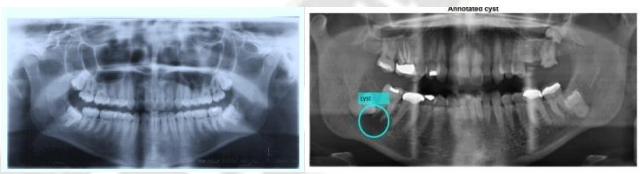

(a) Original (b) Segmented

Figure 2 Original and segmented image of the panaromic images

3.1.3. Model Training

In the model training, it was decided to train two models of convolutional neural networks, to verify which one had better results, and, from this, to be able to choose the best one to export and implement it to the system, which is verified in the validation phase. CNN models used in image classification, such as VGG or LeNet, obtain high precision in their predictions due to their depth (high number of layers). On the other hand, the greatest number of layers produces the

International Journal on Recent and Innovation Trends in Computing and Communication
ISSN: 2321-8169 Volume: 11 Issue: 10
Article Received: *16 August 2023* ***Revised:*** *18 September 2023* ***Accepted:*** *20 October 2023*

phenomenon called gradient fading. For this reason, it was decided to use in this work the two residual CNN architectures most used in the literature: ResNet50 and ResNet101. And these have the particularity that not all the layers are necessarily connected sequentially, some layers are associated with others, skipping intermediate layers relying on a residual function.

• ResNet 50 model

In the model, the architecture of the ResNet50 model offered by the tensorflow library has been used, in which it is loaded with already trained weights offered by Imagenet, for this case the fully connected layers that are typical of ResNet50 for classification were disabled, such as shown in Figure 3, and additional layers were added for the classification of the images, as can be seen in Figure 4.

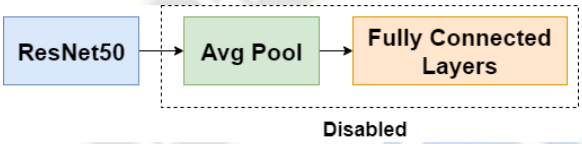

Figure 3 ResNet50 Architecture

Figure 4 shows the structure of the architecture developed for the ResNet 50 model, a model that consists of the aforementioned layers, typical of ResNet 50, and that Additionally, their own will be added to improve the results of the training. First of all, a Flatten layer has been added, which will help to resize the layers bringing them to a single one (flatten). Subsequently, 3 Dense layers with "ReLU" activation function and 3 Gaussian Noise layers will be added that will be used to mitigate overfitting (a form of random data augmentation). Finally, a Dense layer with "softmax" activation function will be added for image classification.

The first dense layer receives as input a space with dimensionality 163840 and outputs a space with dimensionality 2048, the second dense layer outputs dimensionality 512, the third dense layer outputs dimensionality 128, and the last dense layer outputs a dimensionality 163840. output with dimensionality 2, since there are 2 classes of images.

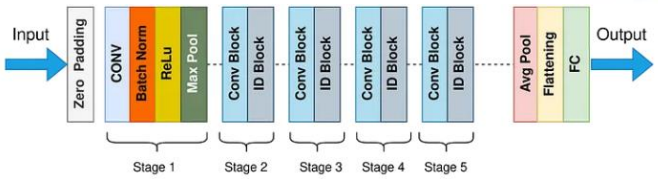

Figure 4 Model architecture using ResNet50

Regarding the compilation of the model, arguments that will be mentioned below were used. First, the Optimizer, configured with a "RMSprop (learning_rate=1e- 2)". Additionally, the Loss Function, configured with "categorical_crossentropy". Finally, the Metric given as "accuracy".

In Figure 5, you can see the results of the accuracy that was obtained after training the model, and its respective test. An average accuracy of 100% accuracy was obtained in the training, but in the case of validation the highest accuracy of 91% was obtained, which is lower, but it is a good result, in addition, it can be observed, in Figure 5, that from season 71 there is a uniformity in training.

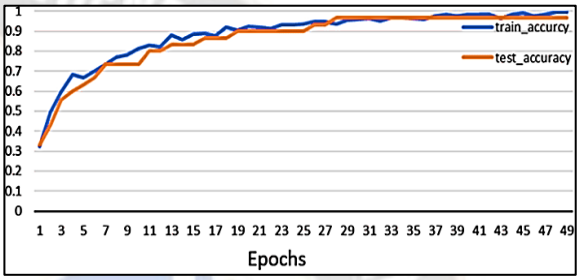

Figure 5 Accuracy of model training and validation using ResNet50

Figure 6 shows the loss obtained during the training and testing of the model. In Figure 6, the loss in training was decreasing during the advancement of the epochs, there is a loss of 0, and, in the case of validation, the loss also had peaks high, but, from epoch 30, it decreased considerably, and it remained so until epoch 100, which varies between 1.5 and 2.

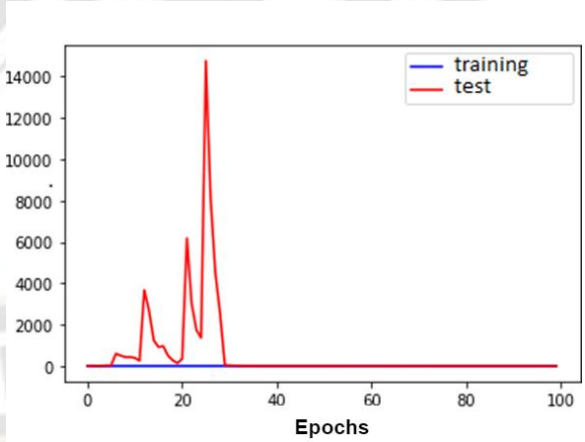

Figure 6 Training loss and model validation using ResNet50

• ResNet 101 Model

In the model, the architecture of the ResNet 101 model offered by the tensorflow library has been used, in which it is loaded with already trained weights that it offers, but, in this architecture, only layer 10 was enabled for training. The fully connected layers that are typical of ResNet 101 for classification were disabled as in ResNet 50, which is why

International Journal on Recent and Innovation Trends in Computing and Communication
ISSN: 2321-8169 Volume: 11 Issue: 10
Article Received: *16 August 2023* ***Revised:*** *18 September 2023* ***Accepted:*** *20 October 2023*

additional layers were added for the classification of the images, as can be seen in Figure 7.

Figure 7 shows the structure of the architecture developed for the ResNet 101 model, a model that consists of the aforementioned layers, typical of ResNet 101, and which will additionally add our own to improve the training results. First of all, a Flatten layer has been added, which will help to resize the layers bringing them to a single one (flatten). Subsequently, 3 Dense layers with "ReLU" activation function and 3 Gaussian Noise layers will be added that will be used to mitigate overfitting (a form of random data augmentation). Finally, a Dense layer with "softmax" activation function will be added for image classification.

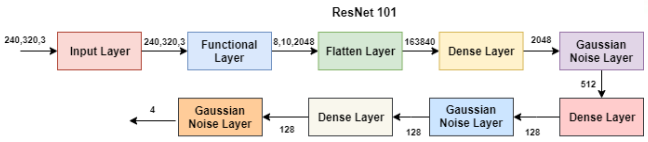

Figure 7 Model architecture using ResNet101

Regarding the compilation of the model, arguments that will be mentioned below were used. First, the Optimizer, configured with a "RMSprop (learning_rate=1e- 2)". Additionally, the Loss Function, configured with "categorical_crossentropy". Finally, the Metric given as "accuracy" For the training, some additional arguments were also used, such as the Batch size, defined with a quantity of 32. The number of Epochs is given as 100.

In Figure 8, you can see the results of the accuracy that was obtained after training the model, and its respective test. An accuracy of 100% accuracy was obtained in the training, but, in the case of the test, the highest accuracy obtained was 89.93%.

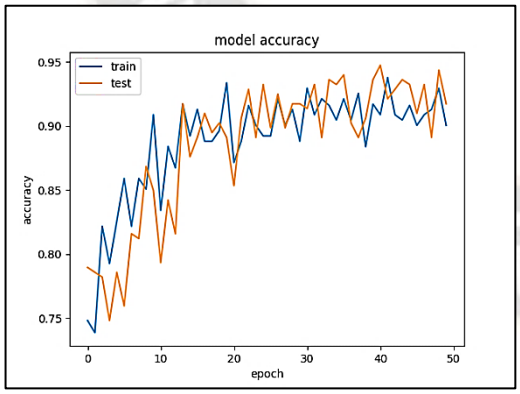

Figure 8 Accuracy of model training and validation using ResNet101

Figure 9 shows the loss obtained during training and testing during model training. In Figure 9, the loss in training was decreasing during the advancement of the epochs, where there is a loss of 0, and in the case of the test the loss was also decreasing, and during the epochs it was stabilizing.

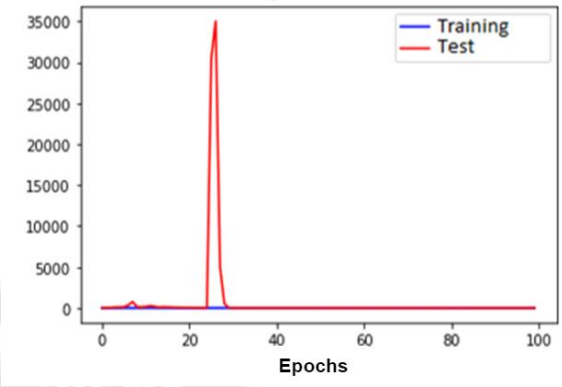

Figure 9 Training loss and model validation using ResNet101

4. Case study

This section describes our population, sample and unit of analysis selected for the research work to different case studies showing the results obtained.

4.1. Population and sample

For the population of the following study, the real-time dataset obtained is considered. In the sample, 150 images from the dataset are considered.

4.2. System validation

In the first instance, the validation of the models used in this research will be carried out. The flowchart of the process of this validation that will be used in the present work is shown in Figure 10.

Precision: It is calculated using the equation (1).

$$precision = \frac{True\ positive}{True\ positive + False\ positive} \quad (1)$$

Recall: It is the number of correctly classified results divided by the number of all samples that should have been classified as positive. It is calculated using the equation (2).

$$Recall = \frac{True\ positive}{True\ positive + False\ negative} \quad (2)$$

Accuracy: It is the ratio between the number of correct predictions and the total number of samples given. This works well only if there is an equal number of belonging samples for each category. It is calculated using the equation (3)

$$Accuracy = \frac{Numarical\ predictions\ \ correct}{Total\ predictions} \quad (3)$$

F1 Score: It is the harmonic mean between Precision and Recall, which tells us how accurate the classifier is, as well as how robust it is. It is calculated using the equation (4)

$$F1 = 2 * \frac{Precison * Recall}{Precision + Recall} \quad (4)$$

International Journal on Recent and Innovation Trends in Computing and Communication
ISSN: 2321-8169 Volume: 11 Issue: 10
Article Received: *16 August 2023* ***Revised:*** *18 September 2023* ***Accepted:*** *20 October 2023*

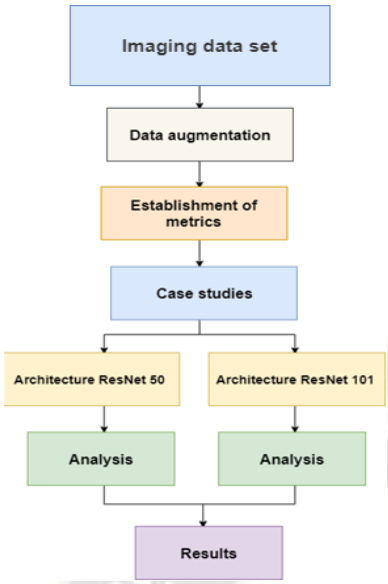

Figure 10 Validation process.

Table 3 shows the number of images with which the validation of the model will be carried out.

Table 3. Number of images by type of classification

Category	Total
Normal	125
Cyst	25

On the other hand, for the validation of the system, 150 images of patients will be used, of which 125 images correspond to normal and 25 to cyst.

4.3. Metrics

According to [31], for the evaluation of the pre-trained models applied, the following metrics will be taken into account.
Precision: It is the number of correctly classified results divided by the number of predicted positive results in the classification.

4.4. Model validation Results

4.4.1. ResNet 50

For this case study, the panaromic images dataset panaromic images dataset divided into four sets of images will also be considered. The pre-trained ResNet 50 CNN model will be applied, the results of the confusion matrix are given in Table 4.

Table 4. Confusion matrix of the ResNet50 model

	Predictions	
	Normal	Cyst
Normal	125	0
Cyst	0	25

- Precision

Classification	True Positive	False Positive	Precision
Normal	123	2	0.984
Cyst	24	1	0.96

The results of precision are given in Table 5.

Table 5. ResNet 50 model precision results

-Recall

The results of recall are given in Table 6.

Table 6. ResNet 50 model Recall results

Clasificacion	True positive	False Negative	Recall
Normal	125	0	1.00
Cyst	25	0	1.00

Based on the data obtained and applying formula (2), the result is that there is a greater recall for the Normal and Cyst category.

- Accuracy

The results of accuracy are given in Table 7.

Table 7. Correct and incorrect predictions of the ResNet 50 model

Classification	Correct predictions	Incorrect Predictions	Total
Normal	123	2	125
Cyst	24	1	25

Given the following data and applying formula (3) as 147/150, an accuracy of 0.98 is obtained, which is a good result, but it does not show that the model is so robust and accurate, since the number of samples is not the same for each category.

-F1 Score

The results of F1 Score are given in Table 8.

Table 8. F1 Score results of the ResNet 50 model

Clasificación	Precisión	Recall	F1 Score
Normal	0.984	1.00	0.99
Cyst	0.96	1.00	0.97

Based on the data obtained and applying formula (4), the result is that there is a higher F1 Score for the Normal category. The opposite occurs with the Cyst category, since an F1 Score of 0.82 is obtained, thus noting that there is a less good classification in this.
In addition, it can be noted that the model is accurate and robust in the classification of the Normal category, and in the case of the Cyst category, the model does not obtain good

International Journal on Recent and Innovation Trends in Computing and Communication
ISSN: 2321-8169 Volume: 11 Issue: 10
Article Received: *16 August 2023* ***Revised:*** *18 September 2023* ***Accepted:*** *20 October 2023*

results, but this would improve if there were more images for this category.

• ResNet 101

For this case study, panaromic images dataset divided into two sets of images will also be considered. The pre-trained CNN model ResNet 101 will be applied. The results of the confusion matrix are given in Table 9.

Table 9. ResNet 101 model confusion matrix Predictions

Classification	Normal	Cyst
Normal	125	0
Cyst	0	25

- Precision

The results of precision are given in Table 10.

Table 10. ResNet 101 model precision results

Classification	True positive	False Positive	Precision
Normal	119	6	0.952
Cyst	23	2	0.92

Based on the data obtained and applying formula 1, the result is that there is greater precision for the category Cyst.

-Recall:

The results of recall are given in Table 11.

Table 11. Results of the Recall of the ResNet 101 model

Classification	True positive	False Negative	Recall
Normal	122	3	0.976
Cyst	25	0	1.00

Table 12. Correct and incorrect predictions of the ResNet 101 model

Classification	Correct predictions	Incorrect predictions	Total
Normal	119	6	125
Cyst	23	2	25

Given the following data and applying formula (3) as 142/150, an accuracy of 0.94 is obtained, which is a good result, but it does not show that the model is so robust and accurate, since the number of samples is not the same for each category.

-F1 Score:

The results of F1 Score are given in Table 13.

Table 13. F1 Score results of the ResNet 101 model

Classification	Precision	Recall	F1 Score
Normal	0.96	0.97	0.96
Cyst	0.92	1.00	0.95

Based on the data obtained and applying formula (4), the result is that there is a higher F1 Score for the Cyst category.

4.4.2. System validation

For the validation of the system, the real time images will be used.

4.5. Analysis of the results

Next, a comparison between both architectures will be made. For this, the analysis previously carried out will be taken into account, where the two aforementioned metrics can be highlighted: Accuracy and F1 Score.

4.5.1 ResNet-50 vs. ResNet-101

Accuracy helps to identify the relationship between the number of correct predictions and the total number of samples given. Table 14 shows the results obtained in both architectures, in which it can be seen that the model based on ResNet50 obtains the best result.

Table 14. Accuracy of ResNet 50 and ResNet 101 models

Architecture	Accuracy
ResNet-50	0.98
ResNet-101	0.94

The F1 Score serves as an indicator to know how accurate and robust the classifier is. Table 14 shows the results obtained in each of the classifications against both architectures, in which it can be seen, in Table 15, that the ResNet-50 pre-trained model yields better results.

Table 15. Comparison of the F1 Score of the ResNet 50 and ResNet 101 model

Architecture	Classification	Precision	Recall	F1Score
ResNet-50	**Normal**	0.98	1.00	0.99
	Cyst	0.96	1.00	0.97
ResNet-101	**Normal**	0.95	0.97	0.96
	Cyst	0.92	1.00	0.95

Evaluating the F1 Score, it can be noted that both models are robust in the Normal, and Cyst classifications, since they have an F1 Score greater than 0.70.

As for the precision for both models, the results are similar, therefore, there is a notable difference, and, as for the Recall, it can be noted that in the Cyst class the ResNet50 model greatly exceeds the ResNet101 model.

Additionally, it can be mentioned that the images, despite only having the categories of Normal and Cyst, can be diagnosed

and provide the current status of the patient. With the support of ResNet50, it is possible to have an accuracy of 0.98, despite the limitations in terms of image quantity and quality. These results can increase if you have the right quantity and quality of images.

5. Conclusions

In the present investigation, a Dental Cyst diagnostic system was developed, where two convolutional neural network models were used: ResNet50 and ResNet101, in which the ResNet50 model obtained a better accuracy. Two models of convolutional neural networks were designed and trained using 80% of the tests, the first based on the ResNet50 model and the second on the ResNet101, of which the one that obtained the best results in the validation phase was the ResNet50 model, with an accuracy of 98%. This model was finally implemented and used in the intelligent system. Additionally, we note that the ResNet101 model also performed well with an accuracy of 94%. These case studies were validated with the following metrics [31]: precision, accuracy, recall and f1-score, the latter two with greater importance since they define that our model based on ResNet50 with the best result is robust.

References

[1] Eriksen, H. M.; Dimitrov, V. The human mouth: oral functions in a social complexity perspective. ActaOdontologicaScandinavica, Taylor & Francis, vol. 61, no. 3, pp. 172–177, 2003.

[2] Mcdonald, S. W.; Macfarlane, N. G. The mouth, stomach and intestines. Anaesthesia & Intensive Care Medicine, Elsevier, vol. 19, no. 3, pp. 128–132, 2018.

[3] Edlund, A.; Santiago-Rodriguez, T. M.; BOEHM, T. K.; PRIDE, D. T. Bacteriophage and their potential roles in the human oral cavity. Journal of oral microbiology, Taylor & Francis, vol. 7, no. 1, pp. 27423, 2015.

[4] IHME. Global Burden of Disease Study 2017. 2018. Disponívelem: <http://ghdx.healthdata.org/gbd-2017>. Acessoem: 17 jul. 2019.

[5] James, S. L.; Abate, D.; Abate, K. H.; Abay, S. M.; Abbafati, C.; Abbasi, N.; Abbastabar, H.; Abd-Allah, F.; Abdela, J.; Abdelalim, A. et al. Global, regional, and national incidence, prevalence, and years lived with disability for 354 diseases and injuries for 195 countries and territories, 1990–2017: a systematic analysis for the global burden of disease study 2017. The Lancet, Elsevier, vol. 392, no. 10159, pp. 1789–1858, 2018.

[6] Kassebaum, N.; Smith, A.; Bernabé, E.; Fleming, T.; Reynolds, A.; Vos, T.; Murray, C.; Marcenes, W.; Collaborators, G. . O. H. Global, regional, and national prevalence, incidence, and disability-adjusted life years for oral conditions for 195 countries, 1990–2015: A systematic analysis for the global burden of diseases, injuries, and risk factors. Journal of Dental Research, vol. 96, no. 4, pp. 380–387, 2017. PMID: 28792274.

[7] S. Kumar, A. Kumar, B. Badiyani, A. Kumar, D. Basak, and M. B. Ismail, "Oral health impact, dental caries experience, and associated factors in 12–15-year-old school children in India," International Journal of Adolescent Medicine and Health, vol. 29, no. 2, 2017.

[8] Listl, S.; Galloway, J.; Mossey, P.; Marcenes, W. Global economic impact of dental diseases. Journal of dental research, SAGE Publications Sage CA: Los Angeles, CA, vol. 94, no. 10, pp. 1355–1361, 2015.

[9] James, S. L.; Abate, D.; Abate, K. H.; Abay, S. M.; Abbafati, C.; Abbasi, N.; Abbastabar, H.; Abd-Allah, F.; Abdela, J.; Abdelalim, A. et al. Global, regional, and national incidence, prevalence, and years lived with disability for 354 diseases and injuries for 195 countries and territories, 1990–2017: a systematic analysis for the global burden of disease study 2017. The Lancet, Elsevier, vol. 392, no. 10159, pp. 1789–1858, 2018.

[10] A. Nowak, J. R. Christensen, T. R. Mabry, J. A. Townsend, and M. H. Wells, *Pediatric Dentistry-E-Book: Infancy through Adolescence*, Elsevier Health Sciences, 2018.

[11] Imran, A.; Jayanthi, P.; Tanveer, S.; Gobu, S. C. Classification of odontogenic cysts and tumors–antecedents. Journal of oral and maxillofacial pathology: JOMFP, Wolters Kluwer–Medknow Publications, vol. 20, no. 2, pp. 269, 2016.

[12] S. Irani and F. Foroughi, "Histologic variants of calcifying odontogenic cyst: a study of 52 cases," *The Journal of Contemporary Dental Practice*, vol. 18, no. 8, pp. 688–694, 2017.

[13] Pontes, C. G. C.; Neto, A. I. T.; Ribeiro, I. L. H.; Sarmento, V. A.; Santos, J. N. D.; Azevedo, R. A. Epidemiology of odontogenic cysts and tumors treated under general anesthesia in a philanthropic hospital in Salvador, Bahia. Journal of Oral and Maxillofacial Surgery and Traumatology, UPE/FO, vol. 12, no. 1, pp. 93–100, 2012.

[14] Costa, F. R.; Esteves, C.; Bacelar, M. T. Benign lesions of the mandible: A pictorial review. ACTA RADIOLOGICA PORTUGUESA, vol. 28, no. 108, pp. 25–35, 2016.

[15] D. Dammerer, J. Neugebauer, D. Putzer, and B. Henninger, "Multiple intraosseouslipomatosis - a case report and a review of the literature," *In Vivo*, vol. 35, no. 2, pp. 959–964, 2021.

[16] J. A. A. de Arruda, L. F. Schuch, L. G. Abreu et al., "A multicentre study of 268 cases of calcifying odontogenic cysts and a literature review," *Oral Diseases*, vol. 24, no. 7, pp. 1282–1293, 2018.

[17] Mikulka, J.; Kabrda, M.; Gescheidtová, E.; Peˇrina, V. Classification of jawbone cysts via orthopantomogram processing. In: IEEE. 2012 35th International Conference on Telecommunications and Signal Processing (TSP). [S.l.], 2012. p. 499–502.

[18] Banumathi, A.; Kannammal, A.; Arthee, R.; Raju, S.; Abhaikumar, V. Automated diagnosis and severity measurement of cysts in dental x-ray images using neural network. International Journal of Biomedical Soft Computing and Human Sciences: the official journal of the Biomedical Fuzzy Systems Association, Biomedical Fuzzy Systems Association, vol. 11, no. 1, pp. 15–19, 2006.

[19] Li, S.; Fevens, T.; Krzyz˙ Ak, A.; Jin, C.; LI, S. Semi-automatic computer aided lesion detection in dental x-rays using variational level set. Pattern Recognition, Elsevier, vol. 40, no. 10, pp. 2861–2873, 2007.

[20] Nurtanio, I.; Purnama, I. K. E.; Hariadi, M.; Purnomo, M. H. Cyst and tumor lesion segmentation on dental panoramic images using active contour models. IPTEK The Journal for Technology and Science, vol. 22, no. 3, 2011.

[21] Vijayakumari, B.; Ulaganathan, G.; Banumathi, A.; Banu, A. F. S.; Kayalvizhi, M. Dental cyst diagnosis using texture analysis. In: IEEE. 2012 International Conference on Machine Vision and Image Processing (MVIP). [S.l.], 2012. pp. 117–120.

[22] Nurtanio, I.; Astuti, E. R.; Purnama, I. K. E.; Hariadi, M.; Purnomo, M. H. Classifying cyst and tumor lesion using support vector machine based on dental panoramic images texture features. IAENG International Journal of Computer Science, International Association of Engineers, vol. 40, no. 1, pp. 29–37, 2013.

[23] Alsmadi, M. K. A hybrid fuzzy c-means and neutrosophic for jaw lesions segmentation. Ain Shams Engineering Journal, Elsevier, 2016.

[24] Birdal, R. G.; Gumus, E.; Sertbas, A.; Birdal, I. S. Automated lesion detection in panoramic dental radiographs. Oral Radiology, Springer, vol. 32, no. 2, pp. 111–118, 2016.

[25] Kishore Sebastian, S. Devi, Innovative method of classification of pulmonary nodules using 3d CNN architecture, Journal of Theoretical and Applied Information Technology, vol.101. no 10, 2023

[26] Poedjiastoeti, W.; Suebnukarn, S. Application of convolutional neural network in the diagnosis of jaw tumors. Healthcare informatics research, vol. 24, no. 3, pp. 236–241, 2018.

[27] Zhang, X.; Zou, J.; He, K.; Sun, J. Accelerating very deep convolutional networks for classification and detection. IEEE transactions on pattern analysis and machine intelligence, IEEE, vol. 38, no. 10, pp. 1943–1955, 2015.

[28] Russakovsky, O.; Deng, J.; Su, H.; Krause, J.; Satheesh, S.; Ma, S.; Huang, Z.; Karpathy, A.; Khosla, A.; Bernstein, M.; Berg, A. C.; Fei-Fei, L. ImageNet Large Scale Visual Recognition Challenge. International Journal of Computer Vision (IJCV), vol. 115, no. 3, pp. 211–252, 2015.

[29] Ariji, Y.; Yanashita, Y.; Kutsuna, S.; Muramatsu, C.; Fukuda, M.; Kise, Y.; Nozawa, M.; Kuwada, C.; Fujita, H.; Katsumata, A. et al. Automatic detection and classification of radiolucent lesions in the mandible on panoramic radiographs using a deep learning object detection technique. Oral Surgery, Oral Medicine, Oral Pathology and Oral Radiology, Elsevier, 2019.

[30] Yong, T.-H.; LEE, S.-J.; YI, W.-J. Odontogenic cysts and tumors detection in panoramic radiographs using deep convolutional neural network (dcnn). 2019.Tharwat, A. Classification assessment methods. Applied Computing and Informatics, vol. 17, pp. 168–192, 2018.